

smaller in these two models to achieve stronger spontaneous emission. To carry the computational burden and guarantee the precision and speed of 3D FDTD method, the adaptive mesh refinement technology has been used in this calculations.

In this study, we have found the influence of the emitter orientation and position on spontaneous emission enhancement, and plot the near electric field distribution of our system. Then we compute the far field directivity of our optical antennas with different particle lengths. It has been found that the emission pattern will not stay dipolar when particle length is large enough. Choosing the incident wavelength of 600 nm, we perform a detailed analysis and comparison of the optical properties of gold nanoparticles.

2. ANTENNA MODELS AND COMPUTATIONAL APPROACH

The plan of our calculation models is shown in Fig. 1, where (a) and (c) stand for PNRs while (b) and (d) for PNEs. all through our calculation, isotropic, linear, and non-magnetic medium is considered. In Fig. 1, each of the nano-rods is made of a cylinder with two hemispherical rounded ends, and *L* is the total length (the height of the cylinder plus the diameter) of one nano-particle. Whereas each nano-ellipsoid is transformed from a sphere by drawing it out in *z* direction and *L* is tip-to-tiplength. For both PNRs and PNEs, *G* is the distance of the gap between two nano-particles, and *R* is the radius of the original sphere. Figs.1(a) and (b) show the electric dipole emitter placed along with the antenna along axis while (c) and (d) show the one placed perpendicular to that. The electronic transition of the quantum emitter is approximated as a pure electrical dipole and represented by a classical dipole.

The analysis has been made using the FDTD method which is simply a space and time discretization of the Maxwell curl equations. Before introducing the calculation approach of decay rates, the dispersion model of metal at optical wavelengths has been discussed.

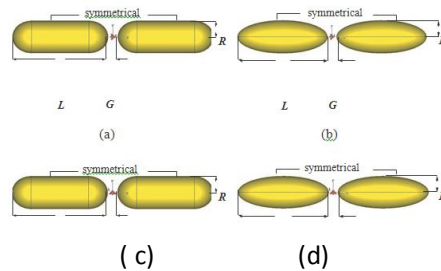


Figure 1. The antenna models designed in FDTD calculation.

Because the perfect conductor approximation is not valid when the metallic nano-structures are studied at visible and near-infrared band, the dispersive negative dielectric function of the metals must be taken into account. And as negative values of ϵ cannot be directly included in the standard set of Maxwell's equations, special techniques are necessary to allow the FDTD calculation to proceed. To simulate gold nano-particles, a modified Drude dielectric function is employed:

$$\epsilon(\omega) = \epsilon_{\infty} - \frac{\omega_p^2}{\omega^2 + j\omega\gamma} \tag{1}$$

where ϵ_{∞} , ω_p and γ stand for the dielectric constant for the frequency going to the infinite, the plasma frequency, and the relaxation frequency of the metal, respectively. For gold, the parameters we used are $\epsilon_{\infty} = 9.5$, $\omega_p = 8.9488$ eV and $\gamma = 0.06909$ eV. A comparison of our fitted Drude model to the bulk values for gold is shown in Fig. 2. The square dots are the real part and the round ones are the imaginary part of the Johnson and Christy bulk dielectric data for gold. While the solid line shows the real part and dashed line shows the imaginary part of our modified

Drude fit. Obviously, in the region of 500–900 nm, our model agrees to the experimental data well. Although BOR technique in the FDTD method can reduce the original three dimensional problem to a two dimensional one, we still cannot use this method in our calculation because our several models do not satisfy the requirements of cylindrical symmetry. As the modeling of the nanostructures requires fine meshes to resolve the geometrical features, mesh size Δs has to be set small enough to insure the accuracy. Moreover, our calculation needs the distribution of the far field to get the Purcell factor, antenna efficiency, and angular directivity. This means the integral region's radius must be more than one wavelength. The simulation domain must be large enough. The calculation regions are 2000 nm * 2000 nm * 2000 nm for both PNRs and PNEs. However, the FDTD mesh has to be limited to a finite region of space to store the field variables and the auxiliary quantities in the computer memory. In other words, to save memory and CPU time, it is convenient to reduce the simulation domain as much as possible. An efficient technology that fulfills the entire requirement mentioned above is the so-called adaptive mesh refinement which we have chosen for our FDTD calculation. More exactly, in our approach, the first step is creating initial mesh. And the minimum grid size plus the maximum one are both set first here, which are 1 nm and 20 nm, respectively. While the electromagnetic field simulation is performed, the energy density in the computation domain is recorded. Regions with high energy density and high field gradients are identified, and the mesh is locally refined there. To mitigate the numerical errors, the ΔS quantity is defined as the maximum deviation of the S -parameters between two subsequent passes. Note that, this deviation is calculated by determining the actual distance between the corresponding curves in the complex plane rather than simply doing a frequency-by-frequency comparison. Small shifts in resonance frequencies therefore cause small differences only. Furthermore a weighting function is applied decreasing the contribution of errors at frequencies further away from the center of the frequency band. The mesh adaptation would not stop until the S -parameters converge such that the ΔS value falls below a certain limit (2% in our calculation). Improving fluorescence of a single emitter with a nano-optical antenna requires systems that deliver a strong local electric field E , a large Purcell factor F , and high antenna efficiency η which is near 100% at the same time.

3. RESULTS AND DISCUSSION

the influence of the electric dipole orientation and position have been compared, followed by the far field directivity analysis. Then the optimization of antenna shape factor to obtain large Purcell factor and high antenna efficiency for both PNRs and PNEs will be discussed in details. This spectrum analysis where incident wavelength varies from 500 nm to 900 nm would be explored. We know, the electric dipole placed in the middle of the gap between two nano-particles has two different orientations. The one is perpendicular to the antenna long axis and the other is parallel to that. Fig. 3 shows the view of the different power flow distributions in $y = 0$ plane, where (a) and (c) are the results of PNRs and the other two belong to PNEs. The electric dipole is perpendicular to the long antenna axis in (a) and (b), while it is changed to be parallel to that axis in (c) and (d). From this figure, both PNRs and PNEs highly confine the power in local field when the emitter orientation is perpendicular to long antenna axis, especially for PNEs. But that power is allowed to radiate to the far field as long as the emitter orientation is parallel to the antenna axis. This could be explained as follows. The nano-particles are in the place where the zenith angle $\vartheta = 90^\circ$ for (a) and (b). According to classical electrodynamics' theory, the magnetic field $H\phi$ must be taken, but when we calculate the average Poynting power, we see

$$\vec{S}_{rav} = \frac{1}{2} \text{Re}(\vec{E} \times \vec{H}^*) = 0 \quad \text{-----}2$$

That means the energy is transforming between the electric form and the magnetic one. So, the field near the antenna is an inductive field, which will not radiate power far. But in the condition of (c) and (d), the zenith angle is changed to be zero. All the magnetic field components are equal to zero.

That means the effect of the magnetic field on the metallic nano-particles can be ignored. Our gold

nano-particles are only influenced by the electric field, which makes positive charges gather in one tip of the nano-particles while free electrons assemble at the other end at the same time. Therefore, these particles can be seen approximately as some newly formed electric dipole emitters with the same orientation as the original one. And they can be very helpful to the enhancement of the spontaneous emission. In the work of Mohammadi displacement of the emitter along the nano-particle axis away from the center was performed. They pointed out this displacement can modify the emission pattern and get stronger enhancement. However, those models are limited to emitters located such that the system preserves cylindrical symmetry. To further discuss the influence of emitter position, we displace the emitter 2 nm away from the nano-particle axis (see the inset of Fig. 4) and compare its Purcell factor and antenna efficiency with those of emitter placed in the center of nano-antenna gap. All these results are shown in Fig. 4, where (a) for PNRs and (b) for PNEs. And we note that, the particle length, radius and gap distance are 80 nm, 20 nm, and 20 nm, respectively.

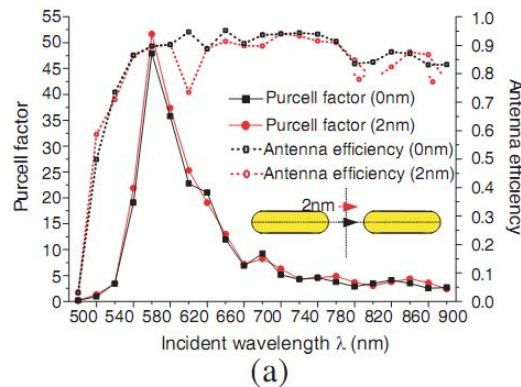


Figure 2. Antenna efficiency η (dashed curves) and Purcell Factor F (solid curves) for an emitter coupled to two gold nano-particles separated by 20 nm for various emitter positions.

Comparing Fig. 4(a) and Fig. 4(b), we can easily find that the PNEs have larger Purcell factors than PNRs at the same wavelength. These results fully accord with the former conclusion drawn by Rogobete and Mohammadi. Moreover, we note that, in Fig. 4(a), the Purcell factor F is larger when we display the emitter 2 nm away from the nano-particle axis. While in Fig. 4(b), that Purcell factor F is smaller. However, there is not much difference for both PNRs and PNEs. As to the antenna efficiency, both (a) and (b) show that η has a decrease if we display the emitter 2 nm away from the nano-particle axis. And this indicates that displacing the emitter will make more power be lost in the metallic nano-particles. In a word, although the displacement of emitter will get larger Purcell factor for PNRs, there is no marked difference in the spectrum from 500 nm to 900 nm. Besides, that displacement will cause greater loss and lower antenna efficiencies. Then, in order to get high Purcell factor and make more efficient optical antennas, we will only discuss those systems with the emitter oriented along the nano-particle axis and just placed in that axis.

4. OPTIMIZATION OF THE GEOMETRICAL PARAMETERS

Several theoretical and experimental realizations have shown that different geometric parameters will change the performance of original electric emitter. In this section, we optimize the geometrical limitations of our nano-optical antenna and want to get larger Purcell factor and higher antenna efficiency. Considering the wavelength of red light which we usually select is around 600 nm, we choose 600 nm as our incident wavelength in the following simulations. First, we note that the Purcell factors for both of the two kinds of antennas decrease as the gap-distance becomes larger. This is because the magnitude of the electric field caused by the dipole emitter is proportional to $1/R^3$. The coupling of the emitter to the

antenna mode will be very weak when the gap is wide enough. Very little power is lost in the metallic nano-particles while most of that is radiated to the far field in the same way as the electric dipole emitter placed in the vacuum. So, in order to get large spontaneous emission enhancement, we must make the gap of two particles be small enough, as long as the manufacture technique permits. However, because of the convenience and accuracy of our simulation, the gap distance is fixed to be 10 nm and no smaller distance is chosen in our following research. We vary the shape factor of each particle by first turning the particle length and then widening the particle radius to further explore the influence of geometrical parameter on emission enhancement and antenna performance. All these results are shown in Fig. 6 and Fig. 3. Fig. 6 is the results when particle radius fixed to be 20 nm while Fig. 3 shows the results of particle length fixed to be 100 nm.

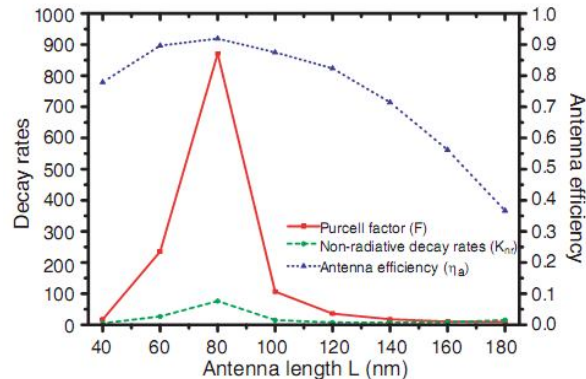


Figure 3.

We first parameterize the shape factor of one particle by the L/R ratio, where L is the length of one particle and R is the radius of that. We find that PNRs has stronger enhancement than PNEs at resonance. That is because the volume of PNRs is larger than that of PNEs when they have same shape factor. Then larger localized field enhancement can be excited. For most settings, PNEs have larger emission enhancement than PNRs with same shape factors. These results fully accord with Rogobete's conclusion that elongated objects should be chosen to benefit from strong near field at sharp corners. And according to the conclusion in Mohammad's work, increasing the shape factor can cause steep decrease of the Purcell factor if the head of the nano-particle is flat. The localized field enhancement is rapidly lost when that kind of particle gets thicker. But we note that, in our calculation, as the length or the radius increases, the radiative decay rates rise to its peak value and then decrease rapidly. Similar trends can be seen for both PNRs and PNEs. Moreover, it should be emphasized that the peak value of the Purcell factor mostly occurs when the shape factor meets the condition of $L/R = 3.5$. What's more, high Purcell factor usually comes with high non-radiative decay rate. But the radiative decay rate is the leading part at resonant which makes the antenna efficiency also stand at high level. Comparing these four figures, we can draw the conclusion that, our optical antenna gets a low efficiency when the shape factor is large enough, especially for PNEs. For example, more than 95% of power is lost in the metallic nano-particles when the PNEs is very thin, where shape factor is $L/R = 10 : 1$. That is because nano-optical antenna with very large shape factor has little plasmon resonance of the antenna lying in this spectral region. Plenty of power is dispersed in the metallic nano-particles. Antenna efficiencies reach higher level and increase more rapidly than the former in shorter wavelength. The long antenna axis L gets larger, the resonance wavelength λR shows a red shift to the near-infrared region. Comparing these results of both PNRs and PNEs, we can find that, the resonance wavelength of PNRs is larger than that of PNEs with the same long axis. For both two types antenna with large aspect ratio, the red shift of PNRs is more evident than that of PNEs. There is a piecewise linearity relationship between the long antenna axis L and the resonant wavelength λR for both PNRs and PNEs and cause huge non-radiative decay rate,

5. CONCLUSION

Two optical antenna models composed of a pair of nano-rods as well as a pair of nano-ellipsoids have been studied. Using the 3D-FDTD method, we have calculated the decay rates and antenna efficiency of an electric dipole emitter coupled to these optical antennas. We first find the right orientation and position of the electric emitter which can radiate the local energy to the far field, cause huge emission enhancement, and have high antenna efficiency. We then perform the far field analysis of both PNRs and PNEs. From those results, we find that the dipolar emission pattern is lost as the particle length reaches 180 nm, and we successfully demonstrate that SPPs excited in the tips of our nano-particles can influence the far field directivity. Choosing the incident wavelength of 600 nm, we carefully examine the influence of shape factor on emission enhancement. Our results show that both PNRs and PNEs will get the largest emission enhancement if their shape factors meet $L/R = 3.5$ we performed the spectrum analysis for both antennas and obtain a piecewise linearity between the long antenna axis and the resonant wavelength. Our results highlight the way of controlling the emitter position and the geometry parameters of the nano-particles to fulfill the experiments requirements, especially when large enhancements are desired. The gold nano-particles have become very attractive for applications in field-enhanced spectroscopy, optoelectronics and active met materials in visible and near-infrared bands.

REFERENCES

1. Kühn, S., U. Hakanson, L. Rogobete, and V. Sandoghdar, "Enhancement of single-molecule fluorescence using a gold nanoparticle as an optical nanoantenna," *Phys. Rev. Lett.*, Vol. 97, No. 1, 017402-4, 2006.
2. Fischer, H. and O. J. F. Martin, "Engineering the optical response of plasmonic nanoantennas," *Opt. Express*, Vol. 16, No. 12, 9144–9154, 2008.
3. Kong, F., K. Li, B.-I. Wu, H. Huang, H. Chen, and J. A. Kong, "Propagation properties of the SPP modes in nanoscale narrow metallic gap, channel, and hole geometries," *Progress In Electromagnetics Research*, PIER 76, 449–466, 2007.
4. Kong, F., K. Li, H. Huang, B.-I. Wu, and J. A. Kong, "Analysis of the surface magnetoplasmon modes in the semiconductor slit waveguide at terahertz frequencies," *Progress In Electromagnetics Research*, PIER 82, 257–270, 2008.
5. Kong, F., B.-I. Wu, H. Chen, and J. A. Kong, "Surface plasmon mode analysis of nanoscale metallic rectangular waveguide," *Opt. Express*, Vol. 15, No. 19, 12331–12337, 2007.
6. Rogobete, L., F. Kaminski, M. Agio, and V. Sandoghdar, "Design of plasmonic nanoantennae for enhancing spontaneous emission," *Opt. Lett.*, Vol. 32, No. 12, 1623–1625, 2007.
7. Mohammadi, A., V. Sandoghdar, and M. Agio, "Gold nanorods and nanospheroids for enhancing spontaneous emission," *New J. Phys.*, Vol. 10, 105015, 2008.
8. Nehl, C. L., H. Liao, and J. H. Hafner, "Optical properties of star-shaped gold nanoparticles," *Nano. Lett.*, Vol. 6, 683–688, 2006.
9. Anger, P., P. Bharadwaj, and L. Novotny, "Enhancement and quenching of single-molecule fluorescence," *Phys. Rev. Lett.*, Vol. 96, No. 11, 113002-4, 2006.